OFFICE OF NAVAL RESEARCH

Contract No. N00014-91-J-1409

Technical Report No. 135

Probing Electrochemical Adsorbate Structure and Reactions with In-Situ Atomic-Resolution Scanning Microscopy: Some Progress and Prospects

by

Xiaoping Gao and Michael J. Weaver

Prepared for Publication

in

Ber. Bunsenge. Phys. Chem.

Purdue University
Department of Chemistry
West Lafayette, Indiana 47907-1393

October 1992

REPORT DOCUMENTATION PAGE

Form Approved
OMB No 0704-0188

1. AGENCY USE ONLY (Leave blank)	2. REPORT DATE	3. REPORT TYPE AND DATES COVERED
	OCTOBER, 1992	

4. TITLE AND SUBTITLE

PROBING ELECTROCHEMICAL ADSORBATE STRUCTURE AND REACTIONS WITH IN-SITU ATOMIC-RESOLUTION SCANNING MICROSCOPY: SOME PROGRESS AND PROSPECTS

5. FUNDING NUMBERS

CONTRACT NO.
N00014-91-J-1409

6. AUTHOR(S)

XIAOPING GAO AND MICHAEL J. WEAVER

7. PERFORMING ORGANIZATION NAME(S) AND ADDRESS(ES)

PURDUE UNIVERSITY
DEPARTMENT OF CHEMISTRY
1393 BROWN BUILDING
WEST LAFAYETTE, IN 47907-1393

8. PERFORMING ORGANIZATION REPORT NUMBER

TECHNICAL REPORT NO. 135

9. SPONSORING/MONITORING AGENCY NAME(S) AND ADDRESS(ES)

DIVISION OF SPONSORED PROGRAMS
PURDUE RESEARCH FOUNDATION
PURDUE UNIVERSITY
WEST LAFAYETTE, IN 47907

10. SPONSORING/MONITORING AGENCY REPORT NUMBER

11. SUPPLEMENTARY NOTES

12a. DISTRIBUTION/AVAILABILITY STATEMENT

APPROVED FOR PUBLIC RELEASE AND SALE; ITS DISTRIBUTION IS UNLIMITED

12b. DISTRIBUTION CODE

13. ABSTRACT (Maximum 200 words)

Some prospects for applying scanning tunneling microscopy (STM) as an in-situ atomic-resolution probe of adlayer structure at ordered metal-solution interfaces are considered with respect to both equilibrium and reactive adsorbate systems. Illustrative results of the former type are presented for the potential-dependent adsorption of iodide at low-index gold electrodes. The virtues of acquiring "composite-domain" STM images, where the electrode potential is altered during data acquisition so to form or remove the adsorbed adlayer, are noted. By generating temporally and spatially adjacent domains featuring substrate and adlayer images in this fashion, the registry between the former and latter atomic arrangements can be deduced with high precision. The suitability of in-situ STM for examining real-space dynamics of surface physical and chemical processes is illustrated for potential-induced reconstruction of Au(100) and for the electrooxidative polymerization of iodide and sulfide. Some limitations as well as strengths of in-situ STM for these purposes are briefly outlined with regard to its anticipated role in the development of in-situ electrochemical surface science.

14. SUBJECT TERMS	15. NUMBER OF PAGES
STM, "COMPOSITE-DOMAIN" IMAGES, ELECTROOXIDATIVE POLYMERIZATION	37
	16. PRICE CODE

17. SECURITY CLASSIFICATION OF REPORT	18. SECURITY CLASSIFICATION OF THIS PAGE	19. SECURITY CLASSIFICATION OF ABSTRACT	20. LIMITATION OF ABSTRACT
UNCLASSIFIED	UNCLASSIFIED	UNCLASSIFIED	UL

Abstract

Some prospects for applying scanning tunneling microscopy (STM) as an in-situ atomic-resolution probe of adlayer structure at ordered metal-solution interfaces are considered with respect to both equilibrium and reactive adsorbate systems. Illustrative results of the former type are presented for the potential-dependent adsorption of iodide at low-index gold electrodes. The virtues of acquiring "composite-domain" STM images, where the electrode potential is altered during data acquisition so to form or remove the adsorbed adlayer, are noted. By generating temporally and spatially adjacent domains featuring substrate and adlayer images in this fashion, the registry between the former and latter atomic arrangements can be deduced with high precision. The suitability of in-situ STM for examining real-space dynamics of surface physical and chemical processes is illustrated for potential-induced reconstruction of Au(100) and for the electrooxidative polymerization of iodide and sulfide. Some limitations as well as strengths of in-situ STM for these purposes are briefly outlined with regard to its anticipated role in the development of in-situ electrochemical surface science.

Introduction

Historically, our understanding of the properties of metal-solution interfaces and the processes that occur there has been developed primarily on the basis of conventional electrochemical methods, i.e. from current-potential-time measurements. In recent years, however, there has been an increasing emphasis placed on supplementing this largely macroscopic information with the more molecular- (and atomic-) level insight obtainable from spectroscopic and microscopic techniques. Surface electrochemical systems present significant challenges to the application of such methods, not the least of which is the presence of bulk-phase interferences arising from the electrolyte solution. These difficulties prompted the development of approaches involving the emersion of the electrode from the electrolyte and transferal into an ultrahigh vacuum (uhv) environment[1]. The usual intent is to remove the bulk-phase solvent while maintaining intact the electrochemical interphase ("double layer"). A related, yet distinct, approach consists of dosing components of the electrochemical system on an initially clean metal surface in uhv[2]. The key virtue of such "ex-situ" tactics is that the surface can then be examined by the wide variety of characterization techniques available in uhv surface science.

Despite the power of these ex-situ methods, the availability of "in-situ" spectroscopic and microscopic methods, where the metal-solution interface is examined under electrode-potential control, has long been recognized as being critical to the development of electrochemical surface science. A progressively larger range of such in-situ methods have emerged in recent years[3]. In several instances, the techniques have been adapted from methods developed earlier (or concurrently) for metal-uhv systems. Besides the advantages thereby gained from a broader base of practical experience and theoretical understanding of such techniques, the evaluation of molecular-level phenomena common to electrochemical

and vacuum-based surfaces provides an important impetus towards establishing a more unified understanding of interfacial science.

Of the various in-situ techniques emerging recently, the one promising to exert perhaps the greatest impact in electrochemical surface science is scanning tunneling microscopy (STM). While STM offers opportunities for exploring real-space surface structure over wide ranges of magnification, undoubtedly of greatest fundamental interest concerns measurements yielding atomic or molecular resolution. The remarkable ability of STM to provide true atomic resolution images (i.e. identification of *individual* surface atoms) was realized for ordered metal-uhv interfaces not long after the initial development of the technique in the early/mid 1980's. Investigations of this type have broadened considerably recently, encompassing the atomic-level imaging of adsorbates as well as the metal substrate[4]. The first reports that atomic-resolution STM images could be obtained reliably at metal-solution interfaces appeared in 1990[5,6]. Since then, an increasing range of studies from several laboratories have begun to demonstrate the power of in-situ STM for elucidating real-space atomic and molecular structure at ordered electrochemical interfaces.

A central research theme in our laboratory involves exploring connections between electrochemical surface structure and reactivity. We make extensive use of in-situ vibrational spectroscopies, specifically infrared and surface-enhanced Raman spectroscopies, in this endeavor. While these techniques yield much insight into structure and bonding for adsorbed species in electrochemical systems, information regarding real-space structural arrangements has been largely unavailable. Although STM so far essentially lacks chemical specificity, the technique might be expected to yield much detailed information on real-space adsorbate structure, especially for adlayers on ordered monocrystalline metals. We have therefore been motivated recently to evaluate STM as an atomic-resolution

probe of adsorbate, as well as metal substrate, structure for both reactive and equilibrium electrochemical systems.

In this conference paper, we discuss some of the immediate prospects for utilizing in-situ STM to obtain information of this type at ordered metal-solution interfaces, illustrated with recent data obtained on single-crystal gold electrodes in our laboratory. While the available examples are rather restricted in scope, they do serve to highlight some strengths as well as limitations of this intriguing new approach to adlayer structure elucidation. In addition to equilibrium interfacial systems, we consider the suitability of in-situ STM for examining surface processes, specifically adsorbate-driven reconstruction and redox-induced chemical transformations. The presentation here is restricted to a relatively brief overview; further details (including experimental procedures, etc.) can be found in the references cited.

Potential-Dependent Adlayer Structures

A topic of longstanding as well as fundamental interest in surface electrochemistry concerns the potential-dependent adsorption of charged species, especially anions. Providing that the adsorption-desorption kinetics are rapid and reversible, the dependence of the adsorbate surface concentration, Γ, on the electrode potential, E, can be established by conventional electrochemical methods. Thus thermodynamic analysis of families of differential capacitance-potential (C_d-E) curves for varying electrolyte concentrations can yield Γ-E data on solid electrodes, including ordered single crystals[7]. Even in the receipt of such analytical information, however, it remains to ascertain the preferred adsorbate binding site(s), if any, and the occurence of ordered adlattice structures which might be expected to form, at least at high packing densities.

Such adsorbate structural information is now commonplace for metal-uhv

systems, resulting largely from low-energy electron diffraction (LEED) measurements[8]. The same technique has also proved useful for some electrochemical systems by using the ex-situ (electrode emersion) tactics mentioned above[1a]. Along with surface X-ray diffraction[9], STM promises to yield spatial structural information for in-situ electrochemical interfaces at a comparable or even greater level of detail. We consider here as illustrative examples the adsorption of iodide on low-index gold electrodes in aqueous solution. These systems provide attractive "test" cases for several reasons, including the strong and markedly potential-dependent adsorption which is encountered along with their suitability for examination by C_d-E measurements[10]. In addition, well-ordered gold surfaces can readily be prepared in laboratory environments by means of flame annealing[10].

Figure 1A shows an STM image of a Au(110) surface in contact with aqueous 10mM KI. The data acquisition consumed about 20 s, the STM tip being rastered slowly upwards from the bottom of the image as shown. The lower portion of the image was obtained with the surface held at a potential of -0.45 V versus saturated calomel electrode (SCE); about halfway up the scan the potential was stepped to 0.1 V. As for other images obtained at potentials negative of ca -0.3 V under these conditions, the lower portion of Figure 1A shows the strings of gold atoms (running diagonally) that are characteristic of unreconstructed Au(110). We have shown earlier that reconstruction to form primarily (1 × 2) domains occurs rapidly on Au(110) in perchloric acid electrolytes at such negative potentials[11]. The observed absence of this reconstruction in iodide electrolytes undoubtedly results from I^- specific adsorption, which is seen to occur on Au(110) in 0.1M KI at potentials positive of ca -1.1 V vs SCE on the basis of C_d-E data[12].

While images showing the Au(110) substrate are reproducibly obtained at

-0.45 V, the upper portion of Fig. 1A, referring to 0.1 V, displays a markedly different pattern that is consistent with the presence of an ordered iodide adlayer. A virtue of "composite-domain" images such as Figure 1A is that the deleterious effects of thermal drift in the piezoelectric drives, yielding distortions in the x-y image and hence uncertainties in the inferred interatomic distances and angles, can be minimized by employing the known substrate atomic pattern as an internal calibration. Moreover, the registry between the substrate and the adlayer atomic arrangements may be determined reliably by mutual extrapolation of the real-space patterns appearing in the lower and upper segments of Fig. 1A. Most clearly, the iodine atoms imaged at 0.1 V are seen to occupy sites in between each parallel string of gold atoms, spaced 4.1Å apart. Detailed examinations of a number of such images yielded the (3 × 2) structure shown in ball-model form in Fig. 1B. Note that a near-hexagonal iodine adlattice is present, with a nearest-neighbor I-I distance of 4.35Å parallel to the Au strings, and a diagonal I-I distance equal to 4.6Å. The adlayer interatomic spacing therefore approaches the lower limit, 4.2-4.3Å, anticipated from the van der Waals diameter of iodine. (Note that the adsorbed iodide should be essentially discharged to yield iodine atoms on the basis of the near-unity electrosorption valency[13].) The iodine coverage, θ_I, is 2/3, based (as usual) on the density of the top-layer gold atoms (8.5×10^{14} atoms cm^{-2}).

Figure 1C provides another example of a composite-domain STM image obtained using the potential-step tactic, for Au(111) in 0.1M $HClO_4$ + 0.5mM KI. The lower portion of the image, at -0.4 V, shows the hexagonal (1 × 1) substrate[15] and the upper portion, at 0.1 V, displays an iodine adlayer having (5 × $\sqrt{3}$) symmetry. As described in ref. 14, this system provides a good example of the value of composite-domain images for obtaining relatively precise adlayer symmetries, utilizing the known (1 × 1) substrate structure to correct for the distorting

effects of thermal drift. Thus the (5 × √3) and related structures can easily be misidentified as the symmetric (√3 × √3) R30° pattern since the former features only a slight (ca 5°) rotation of a pair of iodine rows from the hexagonal arrangement[16,17].

Returning to the Au(110)-I system, the (3 × 2) structure noted above is prevalent only at ca 0.1 to 0.3 V. At lower potentials on Au(110), from ca -0.3 to 0.1 V, a distinctly different pair of iodine adlayer structures are observed. A typical large-scale image of one of these patterns, nonetheless with discernable atomic resolution, obtained on Au(110) in 10mM KI at -0.1 V, is shown in Fig. 2A. Unlike the iodine adlayers in Figs. 1A and B, some significant periodic variation in the "effective height" (z-corrugation) of the iodine adlayer atoms is observed, appearing as variations in the brightness of the spots identified with iodine adatoms. (These images are obtained at constant current, so that greater brightness refers to a higher tip z-displacement.) Such periodic patterns have been observed in STM images for several other metal-I adlayer systems[6,15,17,18] and for metal reconstructions such as on Au(100)[19]. From the data obtained so far, it appears that the relative height (i.e. differences in the z-plane position) of nearby adatoms inferred on this basis can be at least qualitatively reliable. The significance of this information is that it provides another means of deducing adatom binding sites: nearby adatoms displaying higher and lower z-positions can be identified, say, with adsorption in atop and bridging (or hollow) adsorption geometries, respectively.

Another type of system worth mentioning in this context is carbon monoxide adsorbed on Rh(111) and also Rh(110) electrodes. The molecular-resolution STM images of saturated CO adlayers, especially on Rh(111), display noticeable z-corrugations which can be attributed to CO adsorbate present in distinct binding sites[20]. Independent reliable information on the CO binding geometries has

been obtained from in-situ infrared spectroscopy[21]. Intercomparison of corresponding potential-dependent infrared and STM data yielded reliable assessments of adsorbate binding sites as well as adlayer symmetries[20].

Such periodic corrugation patterns in STM images can also provide an additional aid to the assignment of adlattice symmetries, especially for relatively noncommensurate adlayers featuring large and complex unit cells. For example, the near-horizontal rows of iodine atoms seen in Fig. 2A are rotated clockwise by 4.5° from the gold substrate strings. This produces the observed alternations in the atomic z-positions (i.e. the spot brightness) along the above iodine rows every eight atoms, corresponding to periodic variations in the iodine binding sites from fourfold hollow to atop and return as the iodine string traverses each adjacent gold atomic row. (Further details of this and other lower coverage Au(110)-I adlayer structures obtained by in-situ STM will be provided elsewhere[22].)

A related example of an adlayer displaying periodic z-corrugations is seen in Fig. 2B, obtained for Au(100) in 10mM KI at 0.1 V. Slanted strings of more brightly imaged (i.e. higher z-position) iodines are seen, again corresponding to adsorption in near-atop sites, separated by near-hexagonal arrays of more weakly imaged iodine atoms residing in bridging or hollow binding sites. Again, a detailed discussion of the adlayer structure will be available elsewhere[22]. Nevertheless, an interesting feature of this structural pattern worth highlighting here is that the distance between the "slanted iodine strings" increases in near-continuous fashion as the potential is made more positive, corresponding to progressive increases in the iodine coverage[20]. Moreover, variations in the density of this interference pattern are discernable in Fig. 2B along with alterations in the row direction, signaling the presence of slight yet significant differences in the local iodine coverage as well as adlayer

structure within the small (18 × 18 nm) region shown in this image.

Such observations therefore serve to illustrate the power of STM to discern local nanoscale fluctuations in adlayer structure. A more commonly observed example of local structure variations is apparent in the "holes", seen in the Au(110)-I adlayer in Fig. 2A. The presence of such sharp interruptions in the STM adlayer pattern, in particular those corresponding to a single missing atom or defect, are also of value for checking the validity of the images themselves. Thus periodic patterns displaying apparently uniform atomic-resolution structures can often be obtained by probe microscopies which actually correspond to a superposition of images obtained by multiple portions of the tip being simultaneously in suitably close proximity to the substrate surface. Such "multiple tip" (or "blunt tip") imaging can yield false structural information in some circumstances. Conversely, the observation of occasional point defects and related features can provide assurance that such complications are absent, since multiple tip imaging will tend to average out, and hence mask, local structural variations in the observed image.

A comparison of the potential-dependent adlayer structures observed for iodide on the low-index gold electrodes also reveal features of more general interest[14,22]. While iodide binds preferentially in higher-coordination (bridging, hollow) sites at lower coverages, it displays a notable flexibility at higher packing densities. Thus, hexagonal or near-hexagonal iodine adlattices are generally observed, commonly associated with large and complex unit cells featuring iodine bound in a range of site geometries. The compressible nature of iodine adlayers on Au(111) in aqueous solution is also evident from in-situ X-ray diffraction measurements, which demonstrate clearly that the I-I distances in two of the three row directions decrease in near-continuous fashion as the electrode potential is increased[23] (cf Au(100)-I results noted above).

The observation of such ordered halide adlattices, at least by using STM, is limited to electrode potentials where relatively high adsorbate coverages are found, typically within ca 70% of the saturation θ_I value. At lower coverages, the metal substrate is persistently imaged even in the presence of extensive anion adsorption as deduced from C_d–E data. A similar situation also applies to bromide adsorption on gold[22]. It is possible that ordered adlayer structures are still formed at lower coverages, but the adsorbate atoms are too mobile to be imaged by STM. Alternatively or additionally, the adsorbate layer may be disordered ("gas-like") at lower coverages, the ordered ("crystalline") structures observed by STM (and X-ray diffraction) occurring only at high coverages where interatomic packing effects become important. This intriguing question will undoubtedly receive detailed attention in the future.

Real-Space Surface Reconstruction

So far, we have considered adsorbate systems for which the potential-dependent interfacial structures are known (or presumed to be) in equilibrium. At least in principle, however, in-situ electrochemical STM can also be harnessed to explore the real-time and/or real-space dynamics of surface physical or chemical processes. In this and the following section, we consider illustrative examples of applications along these lines.

All three low-index gold surfaces are known to reconstruct in aqueous electrochemical environments at small negative charge densities in a similar fashion to the clean metals in uhv. The original microscopic evidence for potential-induced reconstruction was obtained by electron diffraction following electrode emersion into uhv[24]. More recently, the phenomenon has been examined by several in-situ methods, including second harmonic generation[25] and X-ray diffraction[26] as well as STM[11,19,27]. On Au(111) and Au(100), the kinetics

of reconstruction (and lifting of the reconstruction at small positive electrode charges) can be relatively slow ($\tau_{\frac{1}{2}}$ ~ 5 to 10 min) in electrolytes such as perchloric acid that feature only weak anion adsorption. This enables the occurrence (or lifting) of the reconstruction to be followed by means of real-time sequencies of STM images. In an interesting study of this type for Au(111), Tao and Lindsay were able to evaluate not only the overall potential-dependent reconstruction kinetics but also the spatial fate of the excess gold atoms disposed during the lifting of the reconstruction[27b].

The reconstruction dynamics are markedly more rapid in the presence of adsorbed anions. Thus, for Au(100) in iodide electrolyte, the real-space structural transitions induced by suitable alterations in the electrode potential are essentially instantaneous ($\lesssim$ 0.5 s) on the timescale amenable to conventional STM measurements. This situation nevertheless is convenient for extracting information regarding real-space reconstruction dynamics. Figure 3A is an example of a "composite-domain" image obtained for Au(100) in 10mM KI in a fashion similar to Figs. 1A and C but for a larger surface area, encompassing several terrace regions. The tip was rastered slowly downward. In the upper portion of the image, obtained at -0.55 V vs SCE, parallel corrugations (resembling a ploughed field) are discernable. These undulations reflect the presence of hexagonal surface reconstruction at -0.55 V. Figure 3B shows a closeup atomic-resolution image of the (5 × 27) reconstruction pattern. The large-scale propagation of the reconstruction pattern displays an interesting flexibility allowing the direction of the corrugation rows to deviate significantly from the substrate rows. This enables the reconstruction to circumnavigate surface defects and other imperfections (see ref. 19b for a detailed description). Along with the reconstruction, several pits, about one gold atomic layer (3Å) deep, are evident as "dark" regions in Fig. 3B. These

pits were seen to form along with the reconstruction upon stepping previously the potential in the negative direction; they arise from the need to provide additional gold atoms for the more densely packed hexagonal surface reconstruction.

During the image acquisition, about one-third down Fig. 3A as shown, the potential was stepped from -0.55 to -0.3 V. The additional iodide adsorption thereby created is seen to not only immediately lift the reconstruction, but also to "fill in" the large rectangular-shaped pit that the STM tip was traversing when the potential was stepped. Additionally, several clusters, or ridges, of excess gold atoms are discernable (as small bright regions) on the initially flat, previously reconstructed, Au(100) terrace. These sudden changes in the surface morphology reflect the concerted diffusion of gold atoms required to decrease the surface atomic density by 23% upon lifting the reconstruction. Indeed, examination of a number of such images showed that the gold pits (or ridges) formed in this manner constitute about 20% of the total surface area within large terrace domains. Potential-induced alterations in the position of terrace edges are also seen (as in Fig. 3A), implicating their role as sources or reservoirs of gold atoms. Such STM data can therefore provide valuable information on the nature of surface atom transport associated with reconstruction, and by inference for other physical processes such as localized corrosion.

One other property of the STM images for reconstructed Au(100) is worth noting here. While images displaying clearcut atomic-resolution patterns of the corrugated hexagonal reconstruction as well as the square-planar substrate can be readily obtained (as in Fig. 3B), data obtained at higher gap resistances (i.e. at larger tip-substrate separations) tend to yield milder or even undetectable atomic corrugations for the former structure. This point is

illustrated in Fig. 3C, showing a 20 nm square region of a Au(100) surface held at −0.2 V in 0.1M $HClO_4$ in which both reconstructed and (1 × 1) domains are evident. While the square atomic-level pattern is clearly seen in the latter regions, only the larger-scale undulations are apparent within the former, the hexagonal atomic scale corrugations not being discernable. This observation apparently indicates that the surface electronic wave function on the hexagonal reconstructed surface is distinctly "smoother" than for the (1 × 1) substrate. While further interpretation is unwarranted in the absence of more quantitative observations, the observation nonetheless illustrates the role of electronic, as well as atomic spatial, configurations in determining z-corrugation in STM images.

Surface Chemical Transformations

A central tactic in electrochemistry is the utilization of controlled alterations in electrode potential to trigger surface redox transformations. Such processes range from outer-sphere electron transfer, where the reactant-surface interactions are usually weak and nonspecific, to a diverse array of multi-electron reactions involving chemisorbed species. In-situ spectroscopic, especially molecular vibrational, techniques are contributing importantly to the identification and characterization of such reactive electrochemical adsorbates. The advent of complementary information on the real-space structures for molecular adlayers involved in (or formed by) such processes, as might be provided by in-situ STM, would clearly be of great value and significance.

At first sight, such applications would appear to face major difficulties from the presence of substantial "leakage currents" associated with faradaic reactions at the tip material. In practice, however, such currents can be minimized by careful electrical insulation of the wire forming the STM tip, so

that stable atomic-resolution images can be obtained even in the presence of substantial faradaic electrochemistry at the substrate-solution interface of interest. We briefly discuss here two examples, taken from studies undertaken recently in our laboratory, that illustrate the types of information that can be obtained for electrogenerated molecular adsorbates by this means.

The first case concerns the electrooxidation of iodide on Au(111) to form crystalline iodine/polyiodine films[14]. For the gold-iodine systems as described above, even though the iodide ions are essentially discharged in yielding adsorbed iodine atoms no formal electrooxidation of solution iodide occurs (i.e. no anodic current is passed) at the electrode potentials being considered. However, raising the electrode potential of the Au(111)-I system above 0.2-0.3 V vs SCE yields marked changes in the STM images that are consistent with the electrooxidative formation of adsorbed polyiodide[14]. Figure 4A shows a typical STM image obtained for Au(111) in 0.1M $HClO_4$ + 0.5mM KI at 0.35 V. Short strings of iodine atoms can be discerned. These are loosely organized into hexagonal patterns, but unlike the monoatomic iodine adlayers noted above the close-packed atomic strings tend to lie *along* the gold substrate row directions. The iodine interatomic spacing, 2.9 (± 0.4)Å, is consistent with the formation of linear polyiodide species (I_n^-, n = 3-5), being markedly shorter than the I-I distances noted above ($\gtrsim$ 4.2Å) for the monoatomic iodine layers. Evidence for adsorbed polyiodide formation under these conditions had been obtained previously by surface Raman spectroscopy[28]. The adsorbed polyiodide is seen to be formed by both STM and Raman spectroscopy at potentials significantly below that, ca 0.45 V, corresponding to the onset of continuous iodide electrooxidation, indicating that these species are stabilized significantly by surface interactions[14,28].

Increasing the potential up to the point where anodic current became

clearly detectable, corresponding to multilayer polyiodine film formation, yields dramatic changes in the STM images. Figure 4B shows one example of the rich variety of structures that are observed on Au(111) in these circumstances. The parallel strings of iodines running diagonally in this image lie along one of the $\sqrt{3}$ directions followed approximately by the monolayer iodine structures imaged at lower potentials. This and other pieces of information suggest that these structures act as a template for multilayer film growth[14]. Another interesting feature of the multilayer polyiodide/iodine films is that various surface packing configurations can be observed between regularly spaced "terrace edges", corresponding apparently to various surface crystallographic orientations of the molecular film in an analogous fashion to metal single crystals. More detailed structural studies of the electrogenerated iodine films are planned, especially as a function of the crystallographic orientation of the gold substrate.

The second example of a surface chemical reaction that we have followed at the atomic/molecular level by in-situ electrochemical STM concerns the oxidation of sulfide on Au(111)[29]. At potentials below the onset of sulfide electrooxidation, stable STM images showing a $(\sqrt{3} \times \sqrt{3})R30°$ adlayer of adsorbed sulfur are observed. However, dramatic alterations in the STM images are seen at potentials where the anodic reaction proceeds. An example of such an image, for Au(111) in 0.1M $NaClO_4$ + 0.5mM Na_2S (pH 2.5) obtained at 0 V vs SCE is shown in Fig. 4C. A square-planar array of rectangular-shaped species is evident, replacing the hexagonal $(\sqrt{3} \times \sqrt{3})$ lattice of monomeric sulfur observed at lower potentials. Careful examination of the rectangular structures showed the presence of eight individual tunneling maxima, identified tentatively to individual sulfur atoms, implicating the presence of S_8 species, as might be expected and indeed is implicated from surface Raman spectra for this system[30].

Interestingly, however, the S-S bond distances inferred from the STM

images, 2.3–2.7Å, are significantly longer than those observed in bulk-phase S_8 and other polysulfur species[29]. It appears that such bond distortion occurs so to enable the adsorbed S_8 to become more closely commensurate with the gold substrate lattice. Images obtained for multilayer polysulfur films display more disordered superstructures, with ring dimensions that more closely approximate the bulk-phase species. Consequently, then, the Au–S interactions likely present for the first polysulfur layer act to both order and modify significantly the adsorbate molecular architecture[29].

Some Limitations and Directions

Together with the increasingly impressive range of in-situ STM studies of ordered metal–solution interfaces that are being reported at the present time, we believe that the foregoing examples attest to the power of the technique for extracting atomic-resolution spatial information for electrochemical adsorbates under reactive as well as equilibrium conditions. It is appropriate in this concluding section, however, to reflect on some likely (and even intrinsic) uncertainties and limitations of atomic-resolution STM as applied to electrochemical systems, together with comments on some avenues in which the technique should contribute importantly in the near future.

The most obvious restriction faced by STM, as well by atomic force microscopy (AFM), is that the long ($\leq$ 0.1 s) timescale over which atomic and molecular structural information is obtained requires that the adsorbate remains extremely immobile. This requirement is most readily achieved for high, near-saturated, adlayer coverages where adsorbate–adsorbate interactions will restrict severely surface diffusion. The anticipated preference for adsorbate binding into specific electrode surface sites together with the former factor should yield ordered adlayer structures having well-defined symmetries, as for metal-

vacuum interfaces[8].

Such ordered adlayer structures are exemplified by the low-index gold-iodide interfaces considered above. As already noted, while the iodide adsorbate displays a preference for multifold binding sites, the common occurence of complex (and "fluid") noncommensurate structures reflects the flexibility of the adsorbate coordination geometries in yielding the variable packing densities demanded by the applied electrode potential. The observation of more "discrete" sequencies of potential- (and hence coverage-) dependent adlayer structures might be anticipated for ionic adsorbates having a greater preference for specific coordination geometries. A significant question raised by these considerations is the extent to which the continuous coverage-potential relationships commonly extracted from macroscopic electrochemical measurements reflect the occurence of such flexible (or "fluid") microscopic adlayer arrangements rather than a sequence of more discrete structures, perhaps coexisting in varying proportions as the potential (and hence coverage) is varied. The ability of the STM technique for probing local real-space structural variations may well provide some intriguing information along these lines.

Another interesting issue is the extent that electrochemical adlayer structures may differ from those at metal-vacuum surfaces as a result of the net charges commonly present at the former interfaces. The iodide adlayer systems are probably atypical in that essentially complete adsorbate-metal charge transfer occurs, so that close similarities are expected with uncharged iodine adlayers in related metal-vacuum environments. Adsorbates engaging in more ionic surface bonding, such as chloride, may well yield different adlayer structures that reflect corulombic interactions; such circumstances may also apply at higher positive (or negative) electrode charge densities, where the presence of large diffuse-layer countercharges could modify substantially the inter-adsorbate

interactions. Consequently, then, examining the possible dependencies of the adlayer structures upon the nature of the diffuse-layer counterion would be of substantial value. An interesting example, examined recently by in-situ AFM, concerns underpotential deposited (upd) silver on Au(111)[31]. Markedly different symmetries of the deposited metal adlayer were observed, depending upon the nature of the electrolyte counteranion.

Another likely limitation of STM is that the technique is not expected to yield generally reliable information on height differences (z-corrugations) between structurally distinct adlayer atoms, and especially between adlayer and substrate z-positions. The underlying difficulty, of course, stems from the nature of the electron-tunneling phenomena responsible for the STM images. The measured z-positions refer to the piezo z-displacements required to maintain the tunneling current constant. Since the latter is determined strictly by spatial and energetic orbital overlap rather than merely by the positions of atomic nuclei, one might anticipate that substantial deviations from the "true" atomic z-positions would commonly be observed. For the iodine adlayer systems considered above, however, the observed z-corrugations appear to be semiquantitatively reliable. The same conclusion applies to the corrugated structures formed by gold surface reconstruction[15,19.27]. At least the latter finding is unsurprising since the electronic properties of the gold surface atoms should not be affected greatly by their steric environment.

Serious or even qualitative errors in the interpretation of STM z-corrugations, however, can occur for adsorbates that induce substantial surface electronic perturbations. Thus z-*minima* are both anticipated and observed for adsorbed atomic oxygen under some conditions[4]. Such complications may be more prevalent for molecular adsorbates, even in the absence of strong adsorbate-surface electronic interactions, depending on the ability of the molecule to

assist substrate-tip electron tunneling. Thus the "measured" z-corrugations between the adsorbate and the surrounding substrate atoms should commonly deviate from the actual spatial values, depending on the electron transmission properties of the former. For example, the diameter of adsorbed C_{60} evaluated by z-corrugation STM measurements is about half the actual value, reflecting the imperfect electron-transmitting properties of the fullerene cage[32].

A related factor affecting the interpretation of STM data concerns the oft-observed dependence of the images upon the tunneling conditions, specifically the bias voltage (V_b) and the current (i_t), in that the magnitude of the z-corrugations commonly depend somewhat on both V_b and i_t. A good example is provided by STM images obtained for iodine adlayers on Pt(111), for which the apparent z-corrugation between iodine atoms in adjacent atop and threefold hollow sites increases as the gap resistance R_g ($-V_b/i_t$) is enlarged[33]. Indeed, the latter iodines are no longer visible in the STM images obtained at larger R_g values (i.e. they fail to yield tunneling z-maxima under these conditions). A further complication is that even the appearance of the adlayer structure may depend upon the magnitude and sign of the bias voltage: in some cases the substrate, rather than the adlayer, structure can be imaged at low V_b values[6]. These and related observations probably reflect in part the varying participation of specific adsorbate and substrate orbitals in the electron-tunneling process as the metal Fermi level is altered.

Despite these complications, there appears to be considerable scope in applying STM for the in-situ atomic- and molecular-level characterization of a broader range of electrochemical adlayer systems. The majority of atomic-resolution studies reported so far involve ordered gold surfaces. This reflects in part the relative ease by which gold samples can be handled in air without serious contamination, along with the common use of Au(111) surfaces prepared by

vacuum metal deposition on mica or other suitable templates. The examination of ordered transition-metal electrodes, especially platinum-group metals, is of obvious interest, even though study of these reactive surfaces face greater experimental difficulties given the usual tactics of assembling the STM cell in air. There are very few convincing reports of in-situ STM images of organic electrochemical adlayers, an exception being a recent study of adenine and related biologically relevant bases at the Au(111)-aqueous interface[34]. The strong chemisorption of organic, especially aromatic, molecules at transition-metal electrodes would seem to offer considerable opportunities for in-situ STM characterization. The wide scope of such in-situ studies applied to organic adlayers is particularly evident in the recent STM results of Rabe and coworkers on the dynamic superstructures for physisorbed layers of long-chain alkanes and alkyl derivatives on ordered graphite and metal chalcogenide substrates[35].

Consequently, then, there is ample justification for asserting that in-situ STM should lead to an increasingly profound as well as broadbased appreciation of real-space adsorbate structure and dynamics in ordered electrochemical systems in a similar fashion to the recent, yet better established, applications in metal-vacuum surface science. As for other evolving techniques, the development as well as application of in-situ STM will be facilitated greatly by combining and comparing the experimental data with parallel structural and compositional information extracted from other methods. The comparison of adlayer structural data obtained by in-situ STM and X-ray diffraction would be particularly informative in this regard. Most centrally, however, the combination of in-situ STM with conventional electrochemical measurements should not only aid the development of the former technique but also provide an increasingly firm basis for its application to the elucidation of fundamental electrochemical phenomena. Such prospects provide an exciting vista for electrochemical surface science.

Acknowledgments

This work is supported by the United States Office of Naval Research and the National Science Foundation.

References

(1) See for example: (a) A.T. Hubbard, Chem. Rev., 88, 633 (1988); (b) D.M. Kolb, Z. Phys. Chem., 154, 179 (1987); (c) R. Parsons, in "Comprehensive Chemical Kinetics", Vol. 29, R.G. Compton and A. Hamnett (eds.), Elsevier, Amsterdam, 1989, Chapter 3.

(2) See for example: (a) J.K. Sass and K.J. Bange, ACS Symp. Ser., 378, 54 (1988); (b) F.T. Wagner and T.E. Moylan, ibid, 378, 65 (1988).

(3) See for example: (a) H.D. Abruna (ed), "Electrochemical Interfaces: Modern Techniques for In-Situ Interface Characterization", VCH Publishers, New York, 1991; (b) Other chapters in ref. 1c.

(4) For a review see: J. Wintterlin and R.J. Behm, in "Scanning Microscopy I", Springer Series in Surface Sciences, Vol. 20, H.J. Güntherodt and R. Wiesendanger, eds, Springer-Verlag, Berlin Heidelberg, 1992, Chapter 4.

(5) O.M. Magnussen, J. Hotlos, R.J. Nichols, D.M. Kolb, and R.J. Behm, Phys. Rev. Lett., 64, 2929 (1990).

(6) S.L. Yau, C.M. Vitus, and B.C. Schardt, J. Am. Chem. Soc., 112, 3677 (1990).

(7) For example: G. Valette, A. Hamelin, and R. Parsons, Z. Phys. Chem. (N.F.), 113, 71 (1978).

(8) M.A. Van Hove, S.W. Wang, D.F. Ogletree, and G.A. Somorjai, Adv. Quantum Chem., 20, 1 (1989).

(9) M.F. Toney and O.R. Melroy, in ref. 3a, Chapter 2.

(10) A. Hamelin, in "Modern Aspects of Electrochemistry", Vol. 16, B.E. Conway, R.E. White, and J. O'M. Bockris (eds.), Plenum, New York, 1986.

(11) X. Gao, A. Hamelin, and M.J. Weaver, Phys. Rev. B., 44, 10983 (1991).

(12) See Figure 35 of ref. 10.

(13) D.L. Roth and W.N. Hansen, Surf. Sci., 136, 195 (1984).

(14) X. Gao and M.J. Weaver, J. Am. Chem. Soc., 114, 8544 (1992).

(15) X. Gao, A. Hamelin, and M.J. Weaver, J. Chem. Phys., 95, 6993 (1991).

(16) B.G. Bravo, S.L. Michaelhaugh, M.P. Soriaga, I. Villegas, D.W. Suggs, and J.L. Stickney, J. Phys. Chem., 95, 5245 (1991).

(17) W. Haiss, J.K. Sass, X. Gao, and M.J. Weaver, Surf. Sci., 274, L593 (1991).

(18) B.C. Schardt, S.L. Yau, and F. Rinaldi, Science, 243, 150 (1989).

(19) (a) X. Gao, A. Hamelin, and M.J. Weaver, Phys. Rev. Lett., 67, 618 (1991); (b) X. Gao, A. Hamelin, M.J. Weaver, Phys. Rev. B., 46, 7096 (1992).

(20) (a) S-L. Yau, X. Gao, S-C. Chang, B.C. Schardt, and M.J. Weaver, J. Am. Chem. Soc., 112, 3677 (1991); (b) X. Gao, S-C. Chang, X. Jiang, A. Hamelin, and M.J. Weaver, J. Vac. Sci. Tech., A10, 2972 (1992).

(21) S-C. Chang and M.J. Weaver, J.. Phys. Chem., 95, 5391 (1991).

(22) X. Gao and M.J. Weaver, to be published.

(23) B.M. Ocko et al, to be published.

(24) (a) D.M. Kolb and J. Schneider, Electrochim. Acta, 31, 929 (1986); (b) J. Schneider and D.M. Kolb, Surf. Sci., 193, 579 (1988).

(25) A. Friedrich, B. Pettinger, D.M. Kolb, G. Lüpke, R. Steinhoff, and G. Morowsky, Chem. Phys. Lett., 163, 123 (1989).

(26) (a) B.M. Ocko, J. Wang, A. Davenport, and H. Isaacs, Phys. Rev. Lett., 65, 1466 (1990); (b) J. Wang, B.M. Ocko, A.J. Davenport, and H.S. Isaacs, Phys. Rev. B., in press.

(27) (a) N.J. Tao and S.M. Lindsay, J. Appl. Phys., 70, 5141 (1991); (b) N.J. Tao and S.M. Lindsay, Surf. Sci., 274, L546 (1992).

(28) M.A. Tadayyoni, P. Gao, and M.J. Weaver, J. Electroanal. Chem., 198, 125 (1986).

(29) X. Gao, Y. Zhang, and M.J. Weaver, J. Phys. Chem., 96, 4156 (1992).

(30) X. Gao, Y. Zhang, and M.J. Weaver, Langmuir, 8, 668 (1992).

(31) C-H. Chen, S.M. Vesecky, and A.A. Gewirth, J. Am. Chem. Soc., 114, 451 (1992).

(32) Y. Zhang, X. Gao, and M.J. Weaver, J. Phys. Chem., 96, 510 (1992).

(33) S-C. Chang, S-L. Yau, B.C. Schardt, and M.J. Weaver, J. Phys. Chem., 95, 7559 (1991).

(34) N.J. Tao and S.M. Lindsay, J. Phys. Chem., in press.

(35) (a) J.P. Rabe and S. Buchholz, Science, 253, 424 (1991); (b) S. Buchholz and J.P. Rabe, Angew. Chem. Int. Ed., 31, 189 (1992).

Figure Captions

Figure 1

(A) "Composite-domain" atomic-resolution STM image of (3 × 2) iodine adlayer on (1 × 1) Au(110) substrate in aqueous 10mM KI, formed by stepping the electrode potential from −0.45 V (lower half) to 0.1 V vs SCE (upper half) during image acquisition, scanned upwards.

(B) Ball model of Au(110)–I (3 × 2) unit cell, obtained from STM images as in A. Smaller open circles denote Au substrate atoms, and larger darkened circles the I adlayer atoms.

(C) Composite-domain STM image of (5 × $\sqrt{3}$) iodine adlayer on (1 × 1) Au(111) substrate in 0.1M $HClO_4$ + 0.5mM KI, obtained by stepping from −0.4 V (lower half) to 0.1 V vs SCE (upper half) during image acquisition, scanned upwards (see ref. 14).

Figure 2

(A) Large-scale STM image of iodine adlayer formed on Au(110) in 10mM KI at −0.1 V vs SCE, showing defects and iodine atomic corrugations.

(B) STM image of iodine adlayer on Au(100) in 10mM KI at 0.1 V vs SCE, showing flexible and adjoining corrugated domains.

Figure 3

(A) Large-scale STM image of Au(100) in 10mM KI, showing several substrate terrace regions. Potential was stepped from −0.55 to −0.3 V after ca one-third of downward-rastered scan was completed.

(B) Close-up STM image of Au(100) reconstruction in 0.1M $HClO_4$ at −0.3 V vs SCE (see ref. 19b).

(C) Larger-scale STM image obtained on Au(100) in 0.1M $HClO_4$ at −0.2 V vs SCE, showing corrugated reconstructed segments and adjacent atomic-resolution (1 × 1) domains.

Figure 4

(A) STM image of electrogenerated polyiodide adlayer strands on Au(111), formed in 0.1M $HClO_4$ + 0.5 mM KI at 0.35 V vs SCE (see Ref. 14).

(B) Image of three-dimensional polyiodine film on Au(111), formed following the onset of faradaic iodide electrooxidation (see ref. 14).

(C) Image of close-packed S_8 adlayer, formed on Au(111) in 0.1M $NaClO_4$ + 0.5 mM Na_2S (pH 2.5) after the onset of sulfide electrooxidation (see ref. 29).

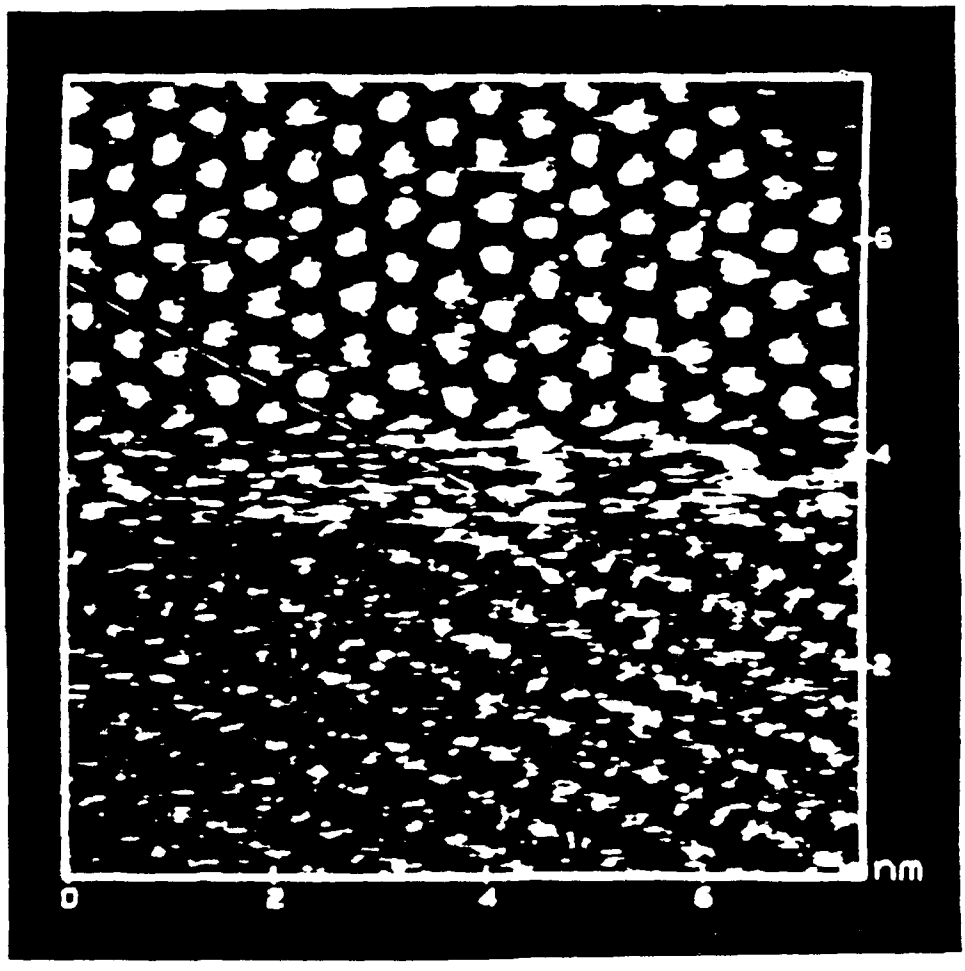

1A

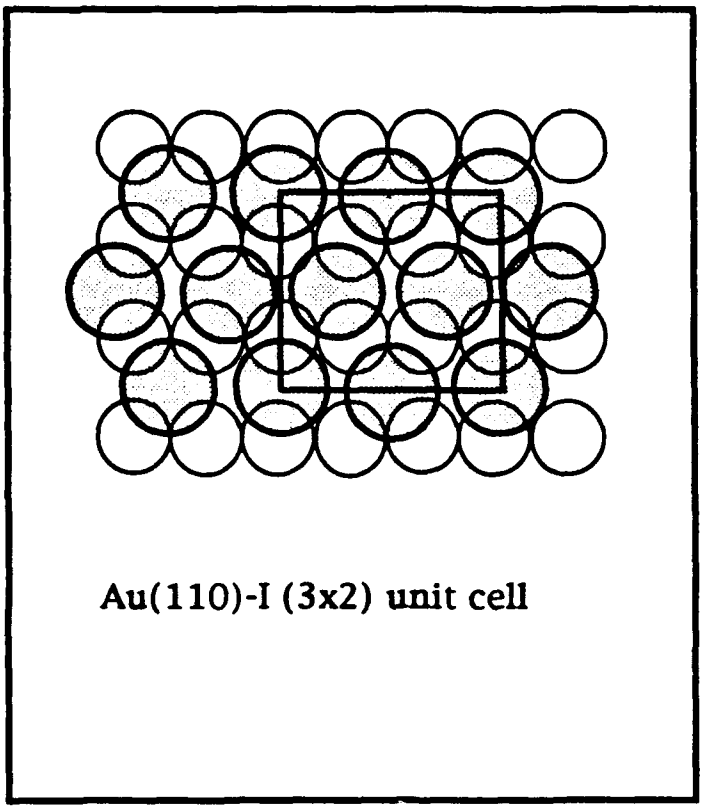

Au(110)-I (3x2) unit cell

1B

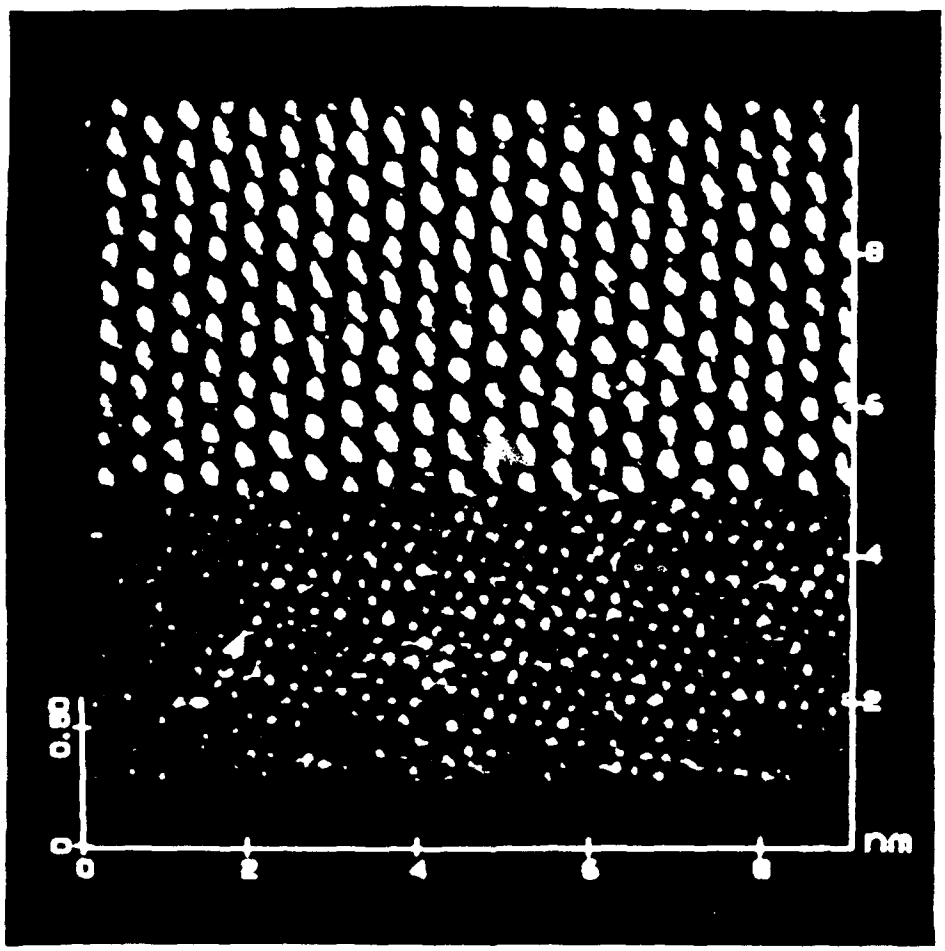

1C

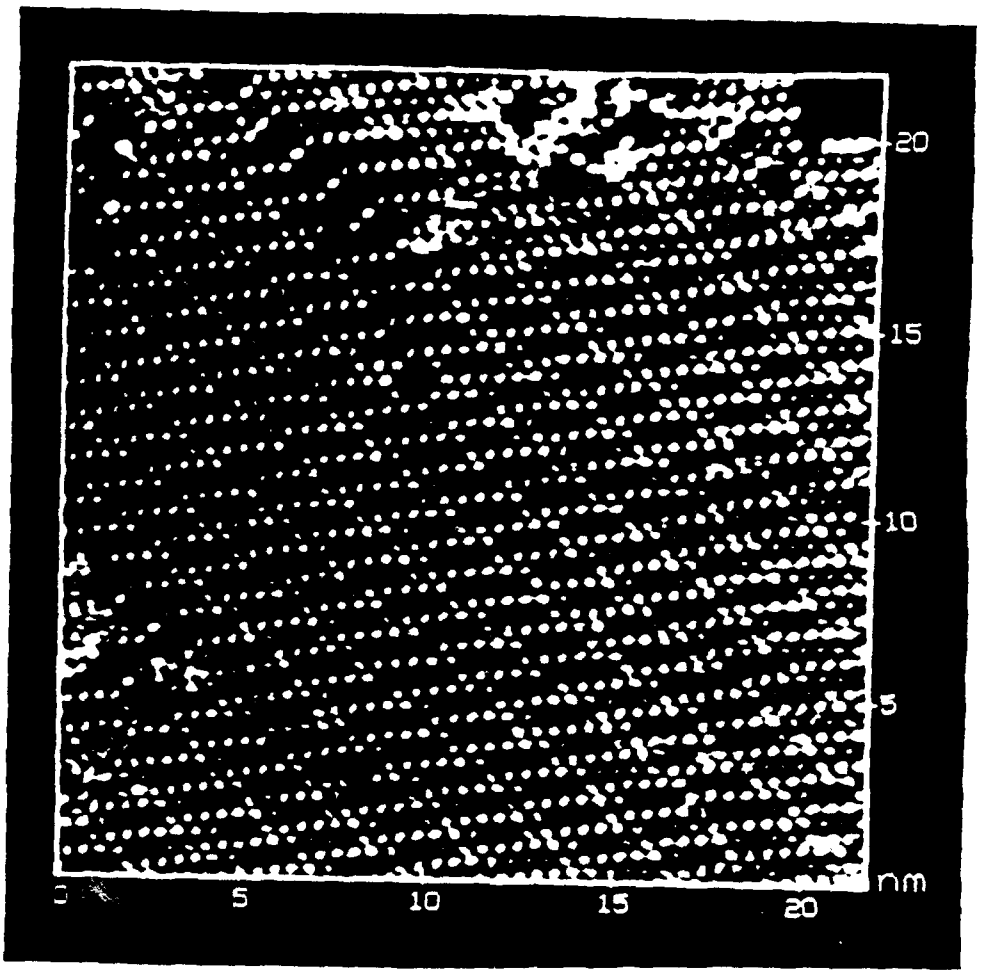

2A

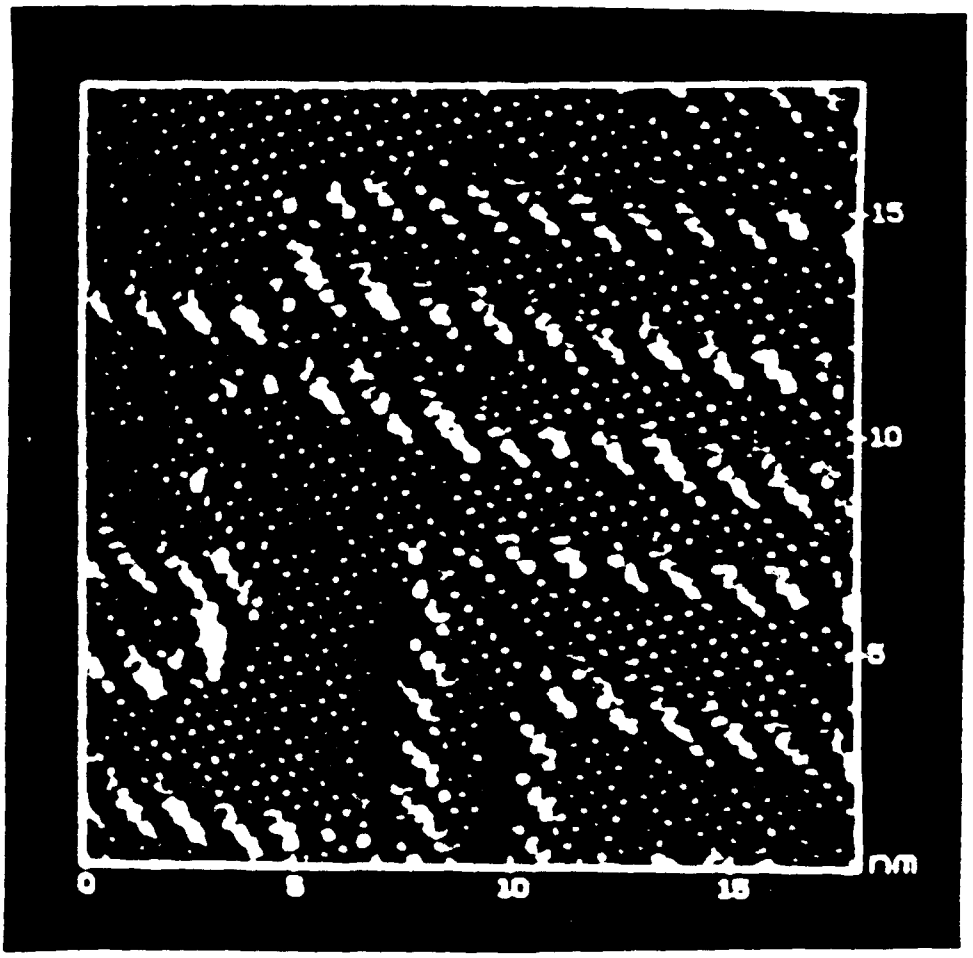

2B

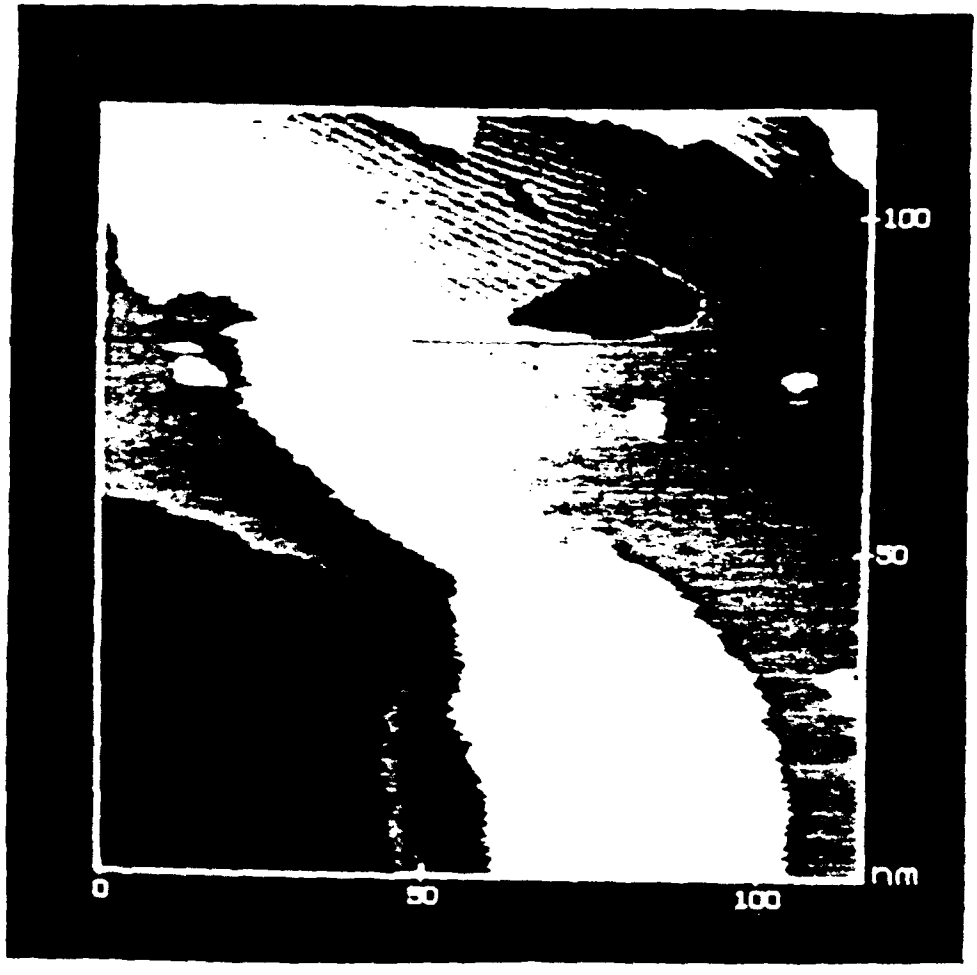

3A

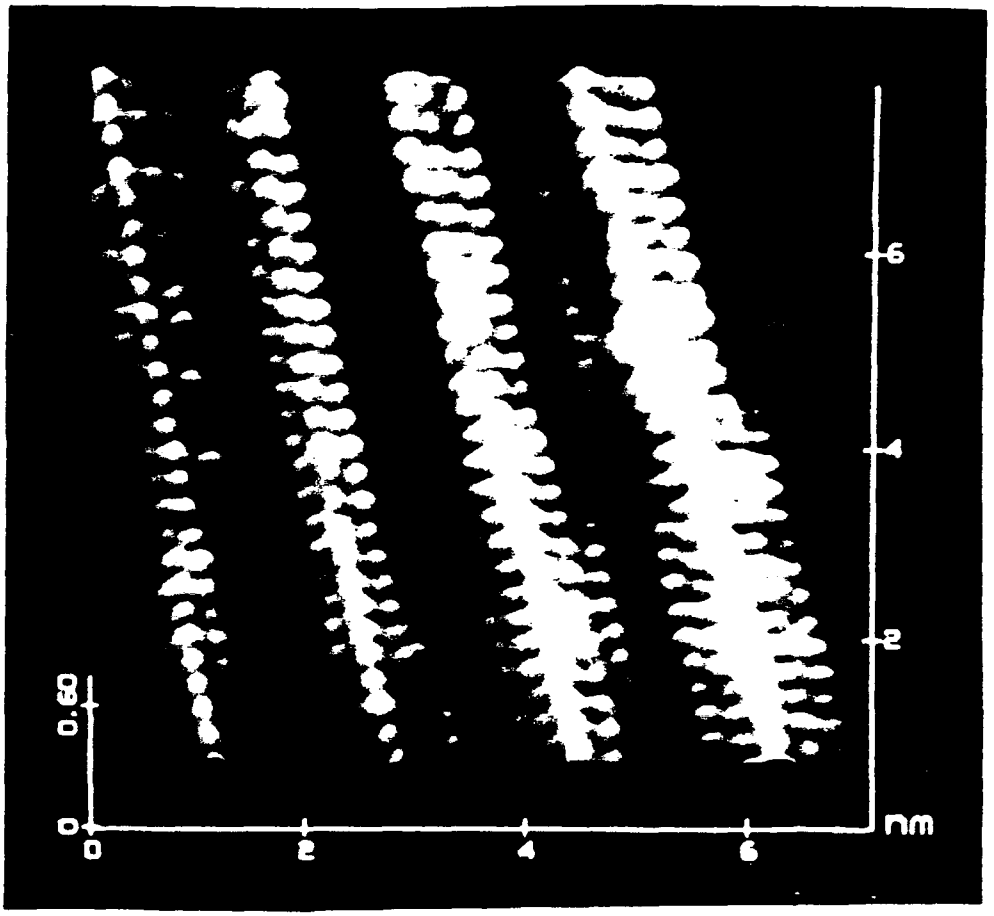
0.60
0
0
2
4
6
nm
6
4
2

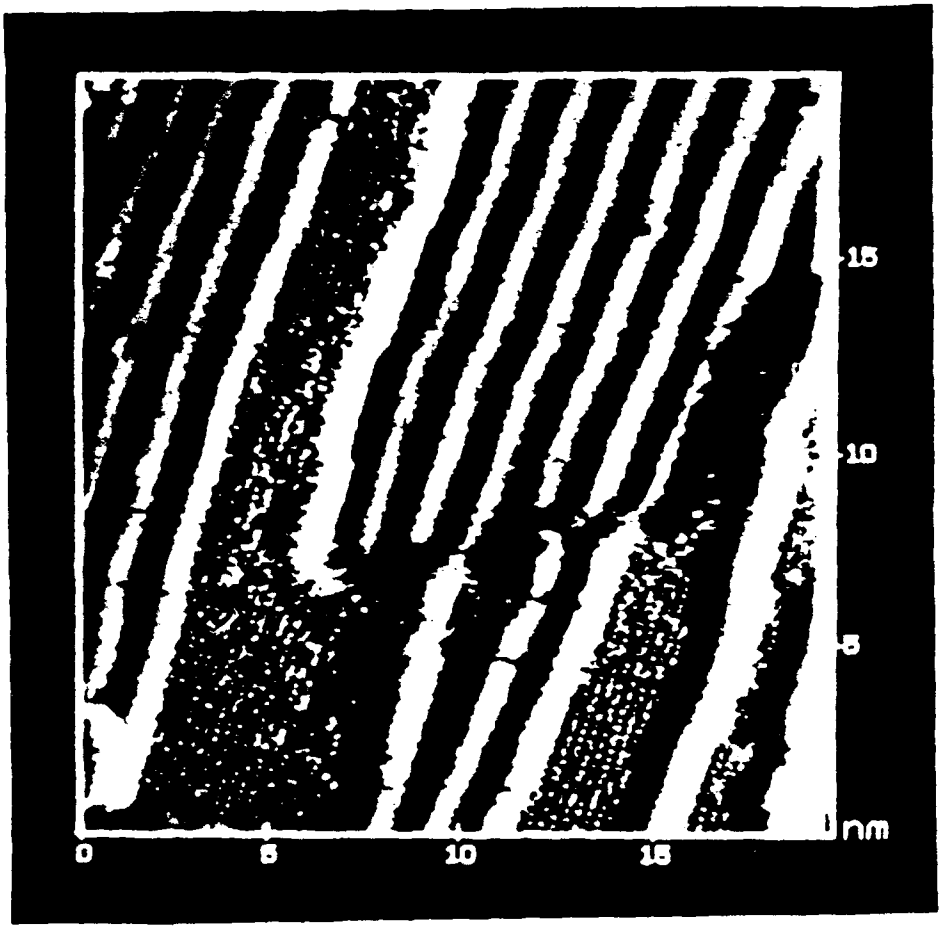

3C

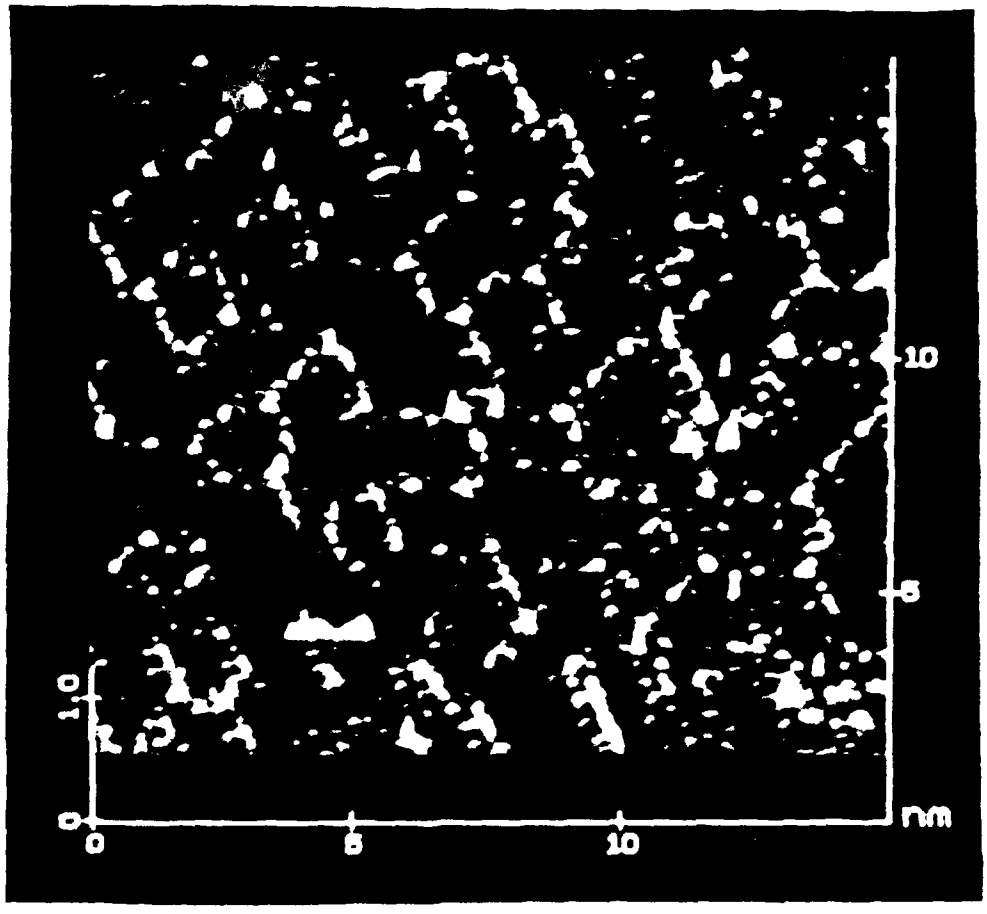

4A

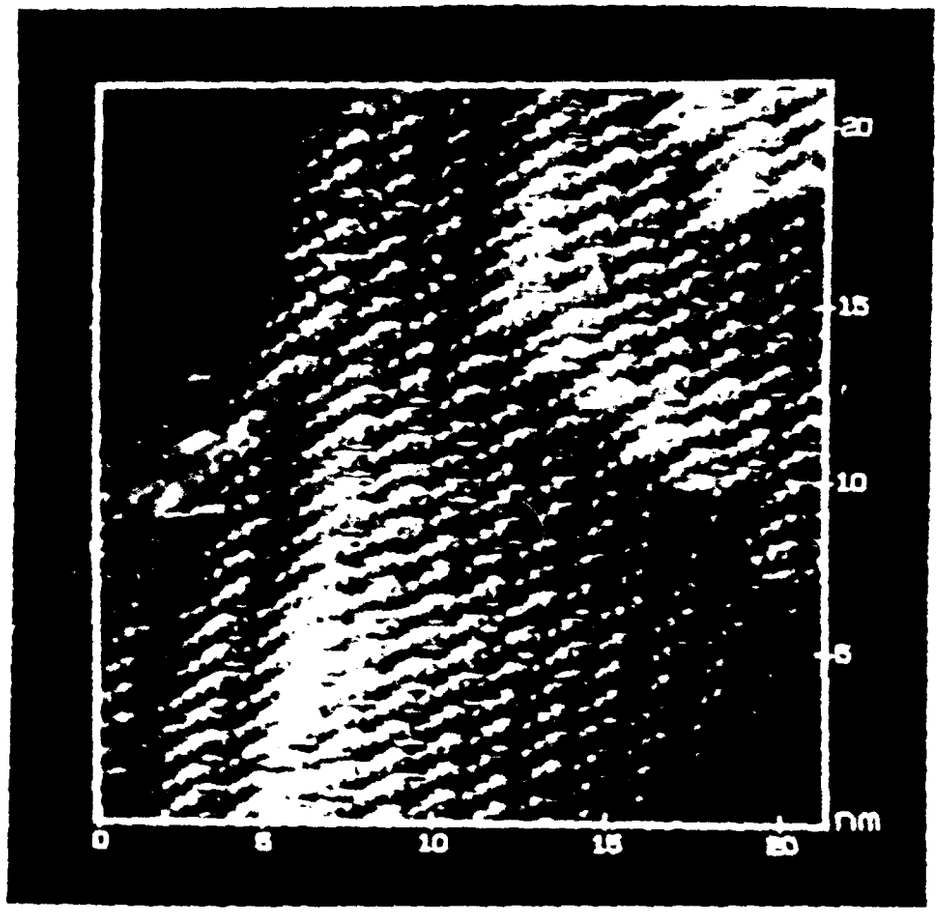

4B

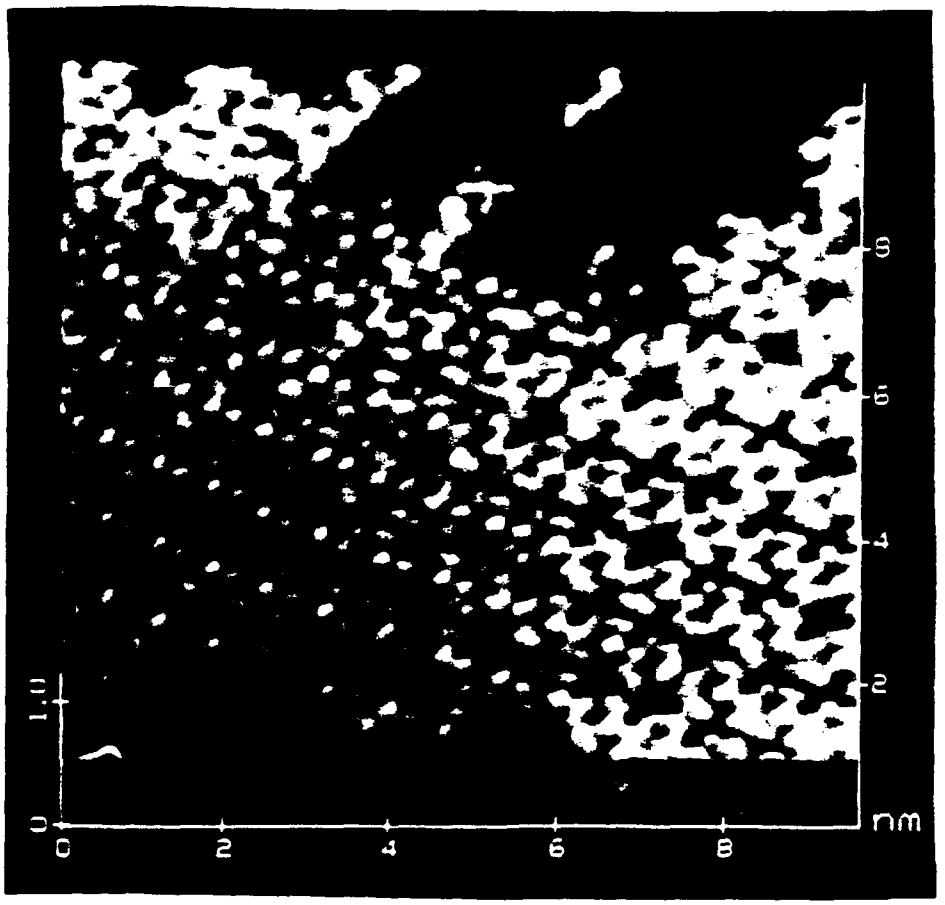

4C